Catalysis Today 187 (2012) 150–158

Contents lists available at SciVerse ScienceDirect

Catalysis Today

journal homepage: www.elsevier.com/locate/cattod

Study of the deactivation of copper-based catalysts for dehydrogenation of cyclohexanol to cyclohexanone

Ernesto Simón, Juana María Rosas, Aurora Santos, Arturo Romero*

Dpto Ingenieria Quimica, Facultad de Ciencias Químicas, Universidad Complutense Madrid, Ciudad Universitaria S/N, 28040 Madrid, Spain

ARTICLE INFO

Article history:
Received 15 July 2011
Received in revised form 5 October 2011
Accepted 11 October 2011
Available online 9 November 2011

Keywords:
Cyclohexanol
Cyclohexanone
Dehydrogenation
Copper
Deactivation

ABSTRACT

Catalytic dehydrogenation of cyclohexanol was carried out in the gas phase in a continuous fixed bed reactor under atmospheric pressure. Two commercial catalysts composed by copper chromite and copper zinc oxide were tested. The activity of the catalysts was evaluated at 250 °C, with a weight hourly space velocity of 2.89 h^{-1} and at times on stream (TOS) higher than 400 h. A slow deactivation of the catalysts was observed during the reaction, obtaining an activity reduction of 50% at TOS = 350 h, but maintaining 30% conversion at these conditions. Yield higher than 97% to cyclohexanone was obtained with both catalysts, in all the range of TOS studied. The main impurity observed was phenol, obtained from dehydrogenation reaction, and cyclohexene, only obtained with the copper chromite catalysts, and derived from cyclohexanol dehydration. The results of stability and selectivity with these catalysts are better than others reported in the literature. The main causes of the activity loss are associated to the coke deposition over the copper active sites and the increase of the copper metallic crystallite size. The copper zinc oxide also presents a slight blockage of the porous structure due to coke deposition, what can also decrease the catalyst activity.

1. Introduction

Cyclohexanone is an important intermediate of the chemical industry. Among its different applications, cyclohexanone is used as raw material for caprolactam manufacture, which is the monomer of nylon 6. Cyclohexanone is mainly produced through the catalytic dehydrogenation of cyclohexanol. From an industrial point of view, the heterogeneous catalytic gas-phase dehydrogenation, at atmospheric pressure, is severely restricted by highly endothermic reaction (ΔH = 65 kJ/mol) and thermodynamic equilibrium [1,2].

Two different conditions for the catalytic dehydrogenation of cyclohexanol can be considered depending on the reaction temperature used: at low temperature, from 200 to 300 °C; and at high temperature, from 350 to 450 °C. Furthermore, two different kinds of catalysts can be used to produce this reaction: copper-based and zinc calcium oxide catalysts, respectively. Recently, most of the studies are carried out with catalysts based on copper formulations. They present a highly dispersed copper phase, when they are carefully reduced; and they usually operate under mild conditions (200–300 °C) [3–7]. These copper catalysts are not used at high temperature due to copper sintering [8]. Metals such as Zn, Cr, Fe, Ni, alkali metals, alkaline earth metals, and thermally stable metal oxides (Al, Si, and Ti) are added to the copper catalysts to enhance their properties. Among the different additives, chromium oxide is frequently used, because it acts as a structural promoter, increasing the BET surface area and also inhibiting the sintering of copper particles [9,10]. The addition of ZnO is also very useful because it promoted the dispersion and stability of the resulting copper catalysts [11,12].

The cyclohexanol dehydrogenation reaction has been widely studied in our research group. In previous papers, we have focused on the identification of the different impurities obtained in this reaction, formed in the transformation stages of the reagents (oxidation, hydrogenation, dehydrogenation, oximation, Beckmann rearrangement, etc.), which affect seriously the final fibber properties; and on the proposal of a kinetic model that describes both the cyclohexanol conversion to cyclohexanone and the phenol production (main impurity of this reaction) [13,14].

Other important factor governing an adequate catalyst selection for an industrial application is deactivation resistance during a long run test. To our best knowledge little works have been published on the deactivation of the copper catalysts for cyclohexanol dehydrogenation reaction. In these works, some of the catalysts tested suffered deactivation, although the authors did not carry out a deep study of the deactivation causes [4,15].

In the present work, we have evaluated the behaviour of two different commercial copper based catalysts on the catalytic dehydrogenation of cyclohexanol, to establish correlations between

* Corresponding author.
E-mail address: aromeros@quim.ucm.es (A. Romero).

0920-5861/$ – see front matter © 2011 Elsevier B.V. All rights reserved.
doi:10.1016/j.cattod.2011.10.010

physicochemical properties and the catalytic activity of calcined, reduced and used catalysts. Furthermore, changes on the catalyst during cyclohexanol dehydrogenation at different times on stream have been also analyzed with the objective to determine the possible deactivation causes (coke depositions, active phase modifications, thermal sintering or physical modifications) [16], as well as the possibility of the catalyst regeneration.

2. Experimental

2.1. Chemical and catalysts

Cyclohexanol (Sigma–Aldrich, 105899), cyclohexanone (Fluka, 29135), phenol (Riedel-de Haën, 33517) and cyclohexene (Fluka, 29230) have been used as reactants or standards. Two commercial catalysts were used: copper chromite catalysts, Cu-0230 (tablets, 3.1 mm × 3.1 mm) supplied by Engelhard, with a weight composition of 72% CuO, 26% $CuCr_2O_4$ and 2% graphite; and copper zinc oxide catalyst, T-2130 (tablets, 3 mm × 3 mm), provided by Süd-Chemie, with a weight composition of 33% CuO, 66% ZnO and 1% graphite. For the sake of simplicity, Cu-0203 is denoted as C1, while T-2130 as C2.

2.2. Catalytic activity

Catalytic dehydrogenation of cyclohexanol to cyclohexanone in the gas phase was carried out at atmospheric pressure in a continuous fixed-bed reactor made of a stainless-steel tube. 10 grams of catalyst are loading in each test. The bed volume was completed with nonporous glass spheres, inert glass wool and stainless-steel wire mesh. As pretreatment, the catalysts were reduced with 95% nitrogen–5% hydrogen at 180 °C for 18 h (gas hourly space velocity, GHSV = 1100 h^{-1}). The reaction temperature was 250 °C. Before the reaction starting, the catalyst was stabilized with N_2 at the reaction temperature. Cyclohexanol was fed with a 5 wt.% cyclohexanone to avoid the cyclohexanol solidification (melting point, m.p. 22 °C). The liquid flow rate was 0.5 mL min^{-1} (weight hourly space velocity, WHSV = 2.89 h^{-1}). The vapour effluent from the reactor was cooled at 20 °C and liquid and gas phase were separated and collected. Liquid phase was subsequently analyzed by GC/FID and GC/MS.

2.3. Catalyst characterization

BET surface area (S_{BET}) and pore volume (V_p) of the catalysts were determined using the N_2 adsorption–desorption technique at −196 °C performed by a Beckman Coulter SA3100 analyzer. Before each measurement, the sample was outgassed at 563 K for 120 min.

The total carbon (TC) was determined by catalytically aided combustion oxidation at 900 °C, with a Co_3O_4 catalyst, using 500 mL min^{-1} of O_2 (99.9 vol.%) as carrier gas, performed by a Shimadzu solid sample combustion unit SSM-5000A.

XRD patterns were recorded on a Philips X'Pert diffractometer, using monochromated Cu Kα radiation (λ = 1.5418 Å), operating at 45 kV and 40 mA. The measurements were recorded in steps of 0.04° with a count time of 1 s in the 2θ range of 5–90°.

The surface chemistry of the samples was analyzed by X-ray photoelectron spectroscopy (XPS) analyses using a 5700C model Physical Electronics spectrometer with Mg Kα radiation (1253.6 eV). For the analysis of the XPS peaks, the C 1s peak position was set at 284.5 eV and used as internal reference to locate the other peaks. Fitting of the XPS peaks was done by the least-squares method using Gaussian–Lorentzian peak shapes.

Infrared (FTIR) spectra were obtained using a Nicolet 5700 spectrometer by adding 256 scans in the 4000–400 cm^{-1} spectral range at 4 cm^{-1} resolution. Pressed KBr pellets at a sample/KBr ratio of around 1:250 were used.

The surface texture of the samples was characterized by scanning electron microscopy (SEM). Scanning electron micrographs were obtained using a JEOL JSM-6400 instrument, working at a high voltage of 20–25 kV.

The solid state ^{13}C NMR experiments were recorded on Bruker Avance-400-WB spectrometers at 100.62 MHz for ^{13}C. Glycine was used as a reference for ^{13}C chemical shifts. ^{13}C CP/MAS NMR spectra were recorded with a spinning rate of 12 kHz, a pulse width of 2.5 μs, a contact time of 5 μs and a recycle delay of 5 s. ^{13}C NMR experiments were conducted with proton decoupling.

The copper metallic surface and dispersion were measured using a nitrous oxide titration method. The sample was in situ reduced with 95/5% of a nitrogen/hydrogen mixture at 180 °C for 18 h, prior feeding N_2O. Afterwards, sample was exposed to pulses of 6.4% N_2O balance with helium at 90 °C. N_2 and N_2O in the exit gas were separated using a PLOT Q column and determined by thermal conductivity detector (Agilent 3000A Micro GC analyzer). A molar stoichiometry $Cu_{sup}{}^0/N_2O = 2$ was assumed, where $Cu_{sup}{}^0$ implies a copper atom on surface.

2.4. Analytical methods

Cyclohexanol and cyclohexanone were analyzed by GC/FID (HP 6890 GC-FID). For this analysis a HP-50+ 19095L-021 (50% phenyl–50% dimethylpolysiloxane) 15 m × 0.53 mm $Ø_I$ × 1 μm column were used. An undecane (Aldrich, U407) was used as ISTD for calibration. Cyclohexene and phenol were analyzed by GC/MS (HP 6890 GC-FID). For this analysis a HP-INNOWAX 19091N-116 (crosslinked PEG) 60 m × 0.25 mm $Ø_I$ × 0.25 μm column were used. A 1,4-benzodioxan (Aldrich, 179000) was used as ISTD for calibration.

3. Results and discussion

3.1. Catalytic activity

Fig. 1 shows the cyclohexanol conversion for C1 (a) and C2 (b) catalysts, at 250 °C and a WHSV = 2.98 h^{-1}. Both copper catalysts presented high initial cyclohexanol conversions. These cyclohexanol conversion values obtained with both catalysts seem to be higher than others reported in the literature with different copper catalysts, however, the experimental conditions and the copper content were not exactly the same [3,15,17]. C1 catalyst showed higher activities than C2, obtaining with both catalysts very high yield (>97%) to cyclohexanone production, as it will be shown in a next section of this work. As it was previously reported, the high catalytic activity observed in the dehydrogenation for both catalysts could be ascribed to the small copper crystallite sizes and the high copper dispersions. Furthermore, the reaction has been also evaluated at 220 and 290 °C, observing steady-state increasing cyclohexanol conversions with the temperature at the same space time [14].

The catalytic activity of both catalysts was evaluated to times on stream (TOS) higher than 400 h. As can be seen in Fig. 1, a reduction of the cyclohexanol conversion, about 50%, is observed for both catalysts at very high TOS (350 h), mainly associated to a partial deactivation of the catalysts. After the observed decreased in the activity, steady state conversions higher than 30% were detected for both catalysts at these high TOS. It is important to point out that, to our best knowledge, the most of the copper catalysts used for cyclohexanol dehydrogenation are only tested at TOS lower than 4 h and only a few authors reported data at higher TOS. Among these studies, the most relevance ones are the works of Krishna

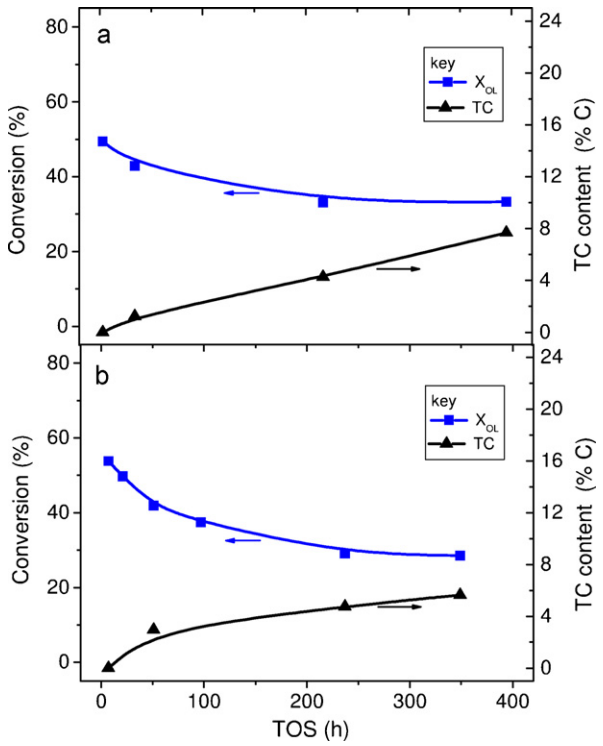

Fig. 1. Evolution of cyclohexanol (X_{OL}) conversion and total carbon content (TC) as a function of TOS for C1 (a) and C2 (b) catalysts. T = 250 °C; WHSV = 2.98 h^{-1}.

Reddy et al. [12], using gamma alumina supported Cu catalysts, they observed stable cyclohexanol conversion at 10 h; Cesar et al. [4], using bimetallic Cu–Co/SiO_2 with different metal loading, they evaluated the stability of their catalysts up to 48 h; and Fridman et al. [7], with Cu–Mg and Cu–Zn–Al catalysts, although they did not show any data at TOS higher than 2 h, they stated that each catalyst was tested for about 170 h, without changes in catalyst activity.

To summarize, an initial deactivation can be observed on both catalysts, obtaining steady state conversions at TOS higher than 200 h. From this point, both catalysts showed a high stability for the cyclohexanol dehydrogenation reaction even at very high TOS. The initial activity decreases can be associated to poisoning, coking, sintering, and/or solid phase transformations. The analysis of the possible causes of deactivation results necessary to take place the study of the regeneration process.

3.2. Chemical properties

XRD. The XRD patterns of the reduced and used catalysts, C1 and C2, are shown in Fig. 2. The copper crystallite size was estimated from Debye–Scherrer equation from the XRD patterns of the catalysts. These data are summarized in Table 1. A more detailed explanation of the characterization of the fresh catalysts was reported in a previous work [14].

C1: The three peaks observed at 43.4°, 50.3°, and 74.1° are characteristic peaks of metal copper crystallite. Wang et al. observed that when the chromium content is below 40%, Cu species mainly exist, in the catalysts, as Cu_2O and Cu^0 [18]. However, the presence of other crystallographic phases of copper, which could be associated to the existence of Cu_2O crystallites, was not detected. In this sense, no signal associated to chromium species has either been observed, suggesting that the species containing chromium and/or Cu_2O could be highly dispersed or exist in amorphous phase.

The XRD profiles of the reduced and used catalysts are very similar, suggesting that the cyclohexanol dehydrogenation reaction does not produce any significant change on the crystalline phases. However, the ratio between the intensities of the peaks associated to the copper crystallite and the intensities of the characteristic peak of carbonaceous species decreases during the reaction, suggesting the formation of coke. Table 1 shows that the copper crystallite size of the catalyst increases approximately a 30% after the reaction at TOS = 395 h.

C2: The XRD pattern of this catalyst shows the presence of metallic copper and ZnO phases. The XRD profile has not been notably affected by the cyclohexanol reaction, in the same way as was observed with C1. However, the crystallite size of metallic copper increases to a great extent with the TOS, from 9 to approximately 27 nm at TOS = 349 h (see Table 1). The ratio between the intensities of the peaks associated to the copper crystallite and the intensities of the characteristic peak of carbonaceous species also decreases during the reaction, probably, as a result of the coke deposition.

Copper dispersion. The copper metal areas are measured by N_2O titration according to the following surface stoichiometry: $N_2O_{(g)} + 2Cu_s \rightarrow Cu_s{-}O{-}Cu_s + N_{2(g)}$. The sizes of copper crystallites and the Cu metal areas of the reduced and used catalysts are also summarized in Table 1. The metallic dispersion of C1 and C2 catalysts determined by N_2O decomposition gave a value of 3.0 and 9.1%, respectively. This value is indicating that metallic phase is formed by large particles of metal copper.

The copper dispersion of the C1 catalyst is slightly decreased after the reaction, due to an increase of the copper crystallite size. However, an important decrease of the surface coverage, about a 45%, is observed at TOS = 395 h. This decrease is related to an increase of the apparent surface area (as shown in Table 3), used for the calculation of the surface coverage. The copper dispersion of the C2 catalyst decreases almost three times after the reaction (TOS = 349 h), increasing significantly the copper crystallite size. It can be seen that the copper crystallite sizes calculated from N_2O chemisorption are higher than those obtained from the XRD data in all cases. In view of these results, the sintering of copper particles seems to be one of the most likely causes of the observed deactivation, mainly in C2 catalyst.

Table 1
Physicochemical properties of the reduced and used catalysts.

Catalyst	Cu surface area[d] (m^2/g)	Cu dispersion[a] (%)	Surface coverage[b]	Cu crystallite size[c,d] (nm)	Cu crystallite size[e] (nm)
C1 reduced	12.6	3.00	0.937	34.5	27.2
C1 used TOS 395 h	11.4	2.71	0.511	38.2	36.2
C2 reduced	15.3	9.06	0.353	11.4	9.0
C2 used TOS 349 h	5.6	3.33	0.151	31.3	24.9

[a] Calculated as the ratio of surface Cu atoms to bulk Cu atoms.
[b] Calulated by dividing the Cu surface area by the BET surface area.
[c] Calculated as: 6000 × (Cu content)/(Cu metal area) × (Cu density).
[d] Determined by N_2O chemisorptions.
[e] Determined by XRD.

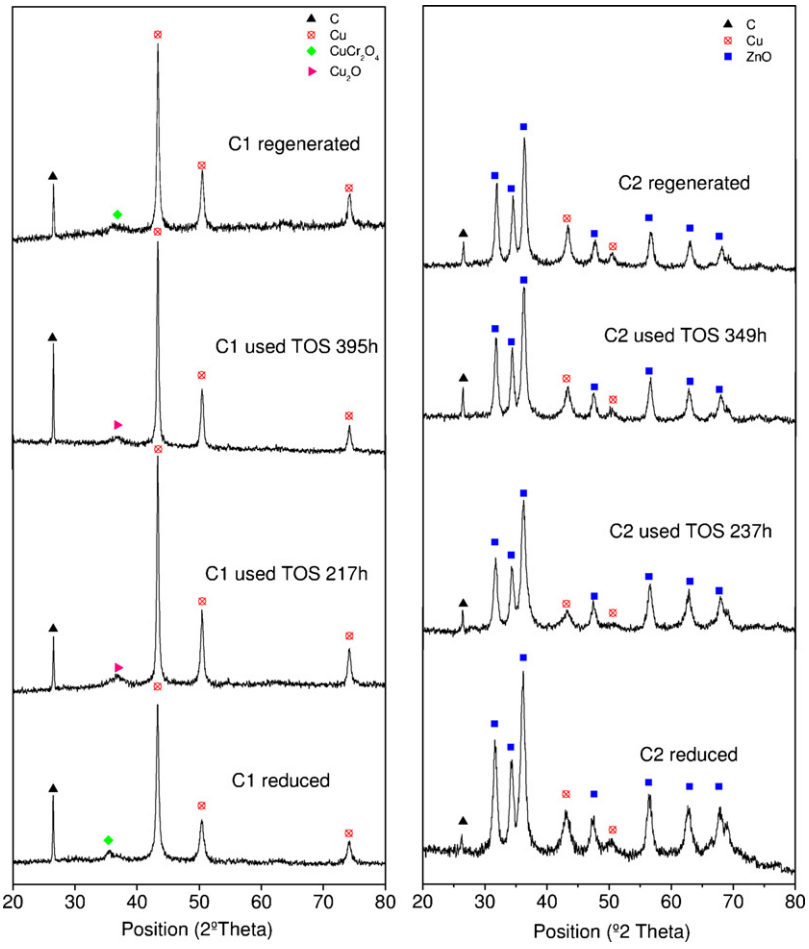

Fig. 2. XRD patterns of the C1 and C2 reduced, used and regenerated catalysts. $T = 250\,^{\circ}C$; WHSV = 2.98 h^{-1}.

3.3. Coke formation

Based on the XRD data, the possible formation of coke was analyzed. Fig. 1 also shows the total carbon content (TC) of the used catalyst as a function of TOS. For the sake of simplicity, this TC corresponds to the total carbon measured after subtracting the initial TC of the catalysts, thus meaning the carbon formed during cyclohexanol dehydrogenation. As can be seen, the carbon content increases with TOS. About 7.67 wt.% coke on C1 catalyst has deposited at 395 h, while about 5.64 wt.% coke on C2 catalyst has been observed at 349 h. This TC increasing tendency of C1 takes place simultaneously to an exponential decay of the cyclohexanol conversion (see Fig. 1), suggesting that the formation of new coke deposits does not produce any significant effect on the catalyst activity. On the other hand, a low coke deposition rate is obtained for C2 catalysts and a pseudo steady state conversion value was obtained at high TOS (>300 h), what suggests that, the decrease on the catalyst activity in C2 can be very influenced by the formation of coke. The coke deposited was analyzed by NMR and FTIR techniques.

NMR. Any significant signal was not observed for the used C1 catalyst at the different TOS studied, probably due to the formation of coke in form of graphite-like or different kind of carbons close to the paramagnetic centres, which are "invisible carbons" by NMR [19]. In fact, some authors proposed that the coke invisible to NMR could be highly condensed polycyclic aromatics or "graphitic" structures [20]. The solid state ^{13}C CP/MAS NME spectra of the reduced and used C2 catalyst at TOS 349 h are shown in Fig. 3. A resonance signal centred between 110 and 150 ppm was observed for the C2 catalyst. This signal can correspond to the formation of carbon atoms with a sp2 hybridized state, which can be associated to polynuclear aromatic compounds. Specifically, the broader line with the greatest intensity at 127.3 ppm can be attributed to non-substituted aromatic carbons of the aromatic rings. While, the weak line at 144.0 ppm, can be assigned to substituted aromatic carbons [21]. Other broad resonance signal was observed between 30 and 50 ppm, which can corresponds to aliphatic carbons.

FTIR. No significant differences were observed between the reduced and used C1 catalyst, only limited to weak and wide bands between 3000 and 2800 cm^{-1}, attributed to C–H stretching bands.

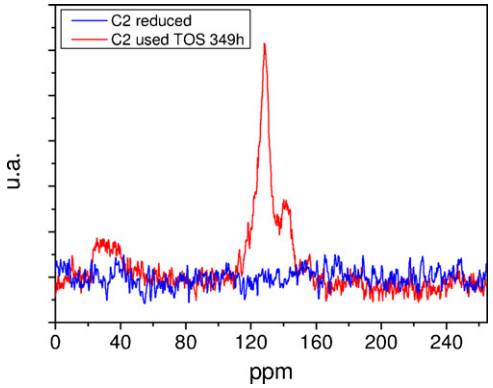

Fig. 3. Solid state ^{13}C CP/MAS NME spectrum of the C2 reduced and used catalyst. $T = 250\,^{\circ}C$; WHSV = 2.98 h^{-1}.

Table 2
Atomic surface concentration of the reduced and used catalysts determined by XPS analysis.

Catalyst	C (%)	O (%)	Cr (%)	Zn (%)	Cu (%)	Cu^{+} (%)	Cu^{2+} (%)
C1 reduced	49.93	34.04	4.45	–	11.58	54.34	45.66
C1 used TOS 34 h	74.65	19.81	2.61	–	2.93	76.5	23.5
C1 used TOS 217 h	74.00	20.11	3.48	–	2.41	88.43	11.57
C1 used TOS 395 h	72.37	21.01	3.64	–	2.98	73.81	26.19
C2 reduced	38.72	36.72	–	18.77	5.8	54.99	45.01
C2 used TOS 51 h	43.07	34.09	–	16.77	6.08	79.42	20.58
C2 used TOS 292 h	48.11	30.84	–	16.39	4.66	93.46	6.54
C2 used TOS 349 h	52.56	28.71	–	14.96	3.77	87.19	12.81

The used C2 catalyst showed the typically absorption bands associated to polycyclic aromatic structures.

At this point, it is important to mention that coke deposition can produce a decrease in the activity of the catalysts by two mechanisms: active site suppression or pore blocking. Both of the two coking modes can occur simultaneously, although one of the two mechanisms is usually predominant. In this sense, the surface chemistry and the textural properties of the catalysts were also evaluated.

3.3.1. Surface chemistry

XPS. Reduced and used catalysts were analyzed by XPS. Table 2 shows the relative atomic surface concentration determined by XPS analysis of these catalysts. As can be seen, the Cu/Cr atomic surface ratio of the reduced C1 catalyst is approximately 2.6. This ratio is lower than the corresponding bulk ratio provided by the manufacturer. In this sense, Guoyi Bai et al. proposed that this is due to Cr is present in a highly dispersed phase on the catalyst surface, which is in agreement with the XRD results [22]. The Cu/Cr atomic surface ratio decreases to values lower than 1 during the reaction, due to an important reduction of the copper content (about a 75%), while the chromium content decreases only slightly. The decrease of the copper content can be observed simultaneously to the increase of the carbon content. These results also suggest the formation of coke, in agreement with the XRD and TC analysis. As aforementioned, this coke deposited can produce the blockage of the pores or maybe the poisoning of the copper active sites. In this sense, the results shown in Table 2 suggest that the partial deactivation of the catalysts can be mainly related to the presence of coke deposited over the copper active sites.

The atomic copper content on the surface of the reduced C2 catalyst is lower than the one observed for the reduced C1 catalyst. The Cu/Zn ratio of the reduced C2 catalyst is approximately 0.3, decreasing to 0.25 at high TOS. In this case, the copper content decreases about a 35%, while the carbon content increases the same 35%, suggesting that coke deposition takes places mainly over the copper active sites in the same way as it occurs with the other catalyst. Although the reduction of the copper active sites due to the coke deposition does not seem as drastic as the one observed with the C1 catalyst.

The chemical oxidation states of Cu in C1 and C2 catalysts at various stages of reaction were also studied by X-ray photoelectron spectroscopy (XPS). The XPS spectra of Cu2p3/2 of the catalysts are shown in Fig. 4(a) and (b), respectively. For the sake of comparison, the XPS spectra of the catalysts before the reduction step were also included (calcined catalyst). The C1 catalyst, before the reduction step, presents a well-separated main peak at 934.5 eV and a satellite peak at 941.5 eV, characteristic of Cu^{2+}. A significant decrease of the satellite peak and a simultaneous shift of the Cu2p3/2 peak towards lower binding energy (BE) are observed after the reduction step, indicating the co-existence of non-reduced and reduced copper species, probably due to an ineffective reduction of the catalyst. A further decrease of the satellite peak was observed during the reaction, suggesting that the reductant atmosphere produced during the cyclohexanol dehydrogenation can provide an additional and more effective reduction of the copper species. As can be seen, the Cu2p3/2 XPS spectra of the catalyst at the different TOS are very similar, what can indicate that steady-state conditions are reached beyond a certain time on stream. For the C1 used catalyst, the Cu2p3/2 band can be deconvoluted into two different peaks. The most important peak is obtained at 932.4 eV, the KE is at 917.3 eV and the modified Auger parameter is about 1849.7 eV. According to the copper chemical state plot, the peak can be attributed to Cu_2O, which means that Cu^{+} is the main copper species (approximately 75%) on the catalyst during the reaction [23]. The relative percentages of the different copper species are also included in Table 2.

The Cu2p3/2 XPS spectrum of the calcined C2 catalyst presents an only peak associated to the presence of Cu^{2+}. After the reduction, the band can be deconvoluted into two peaks, attributed to Cu_2O (76.5%) and CuO (23.5%). In this case, the C2 catalyst also undergoes, during the reaction, an additional reduction with the H_2 produced, obtaining approximately a 90% of Cu^{+}. This percentage remains very similar at the different TOS studied.

The XPS results of both catalysts initially indicate the presence of Cu^{+} as the only non-reduced specie. These results seem to be in

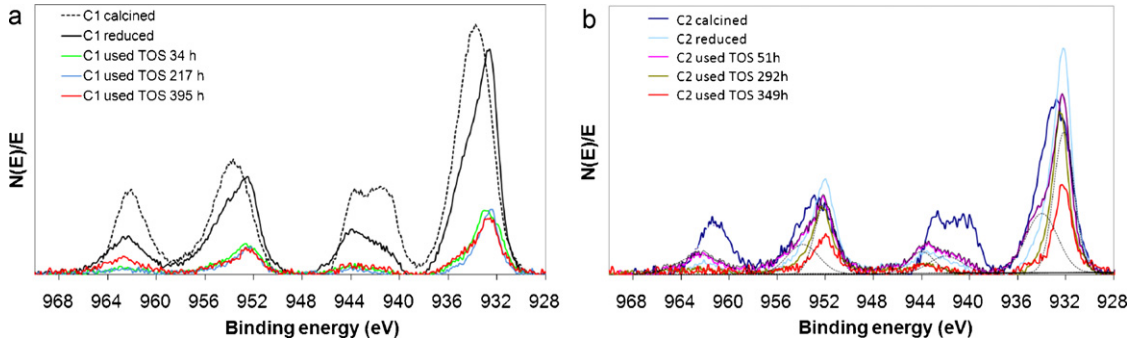

Fig. 4. XPS spectra of Cu2p3/2 of the reduced and used C1 and C2 catalysts. $T = 250\,^{\circ}C$; WHSV = 2.98 h^{-1}.

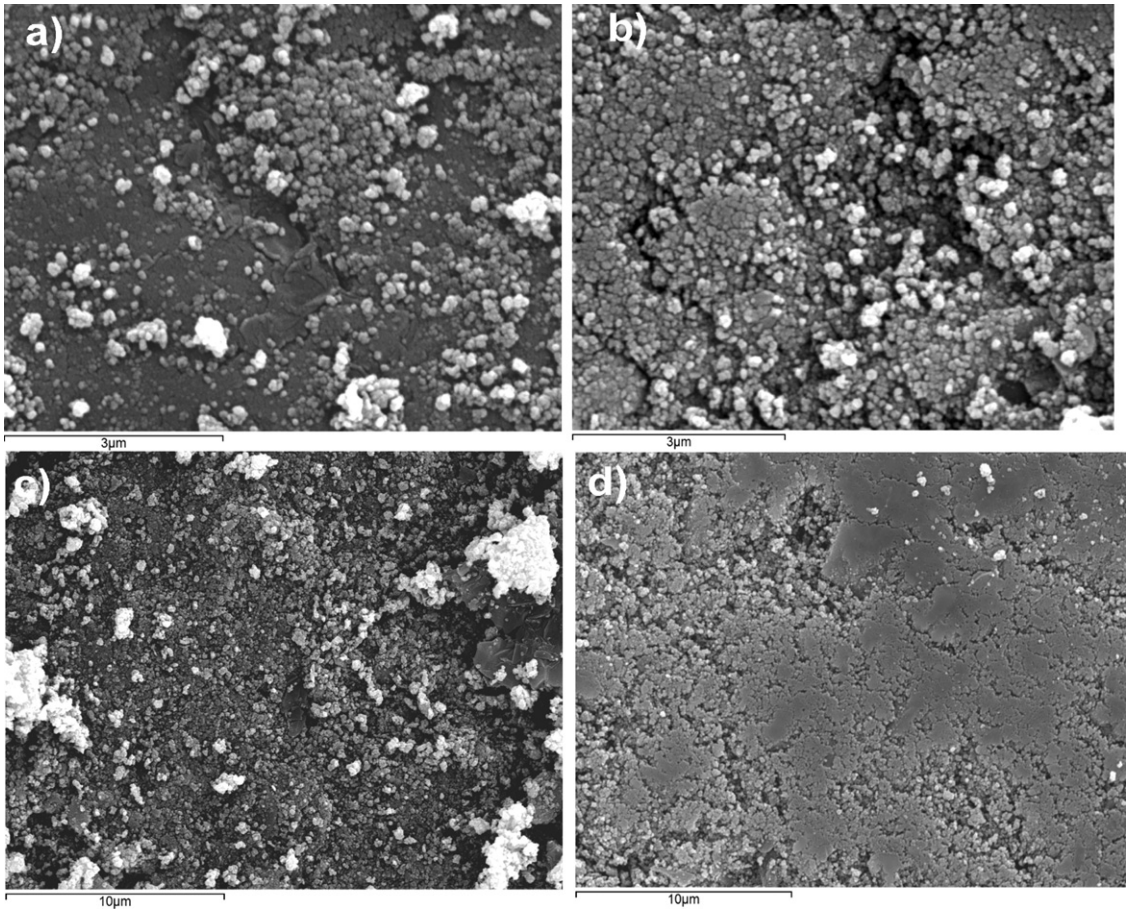

Fig. 5. . SEM micrographs of the C1 reduced (a), C1 used at TOS 395 h (b), C2 reduced (c) and C2 used at TOS 349 h (d) catalysts. T = 250 °C; WHSV = 2.98 h^{-1}.

contrast of the XRD data. However, as aforementioned, XRD data shows the existence or not of crystallographic phases of the different compounds. The results of XRD can indicate that Cu_2O could be present in an amorphous state or highly dispersed. It is also noteworthy that XRD can only calculate crystalline sizes that are larger than 2–5 nm [24]. On the other hand, it is important to mention that Auger spectra, used for the assignment of the chemical oxidation states, have distinctive features for the different copper species, CuO, Cu_2O and Cu. But since they are very broad and close in energy, these Auger spectra have a limited utility when trying to quantify the amount of Cu^{2+}, Cu^{+} and Cu^{0} present in a partially reduced sample. In this respect, the Cu 2p3/2 peak position neither does allow a clear distinction of Cu_2O and Cu [25].

With regard to the active chemical oxidation state of copper for this reaction can be found many works, the most relevant are the works of Fridman and Davydov [5–7], Bai et al. [22] and Wang et al. [23]. Fridman and Davydov [5–7] studied this reaction with Cu–Zn–Al or Cu–Mg catalysts and they suggested that Cu^{+} is more active than Cu^{0}. However, Wang et al. [23] reported a different result, namely that Cu^{0} is the active site for the dehydrogenation of cyclohexanol to cyclohexanone, and Cu^{+} is the active site for the aromatization of cyclohexanol over Cu–Zn–Si catalysts. Based on our own results, the high activity of these catalysts and the low amount of aromatization products obtained seem to be more related to the presence of metallic copper, clearly observed by XRD analyses than the Cu^{+}, as suggested Wang et al. [23].

3.3.2. Textural properties

Table 3 shows the apparent surface area (S_{BET}), the pore volume (V_p) and the mean pore radius of the reduced and used, C1 and C2 catalysts, respectively. The reduced C1 catalyst presents a very low value of S_{BET}, indicative of a poor development of the porous structure. After the C1 catalyst was used for 395 h, its catalytic activity decreased (Fig. 1), however, its BET surface area and pore volume slightly increases. The data derived from the N_2 adsorption-desorption isotherms (not shown) suggest that coke is deposited in the macropores of the catalysts, leading to the formation of wide micropores and mesopores. In this case, the partial deactivation of the catalyst due to the partial blockage of the pores must be ruled out, suggesting that the coke deposition mainly takes place over the copper particles, decreasing the number of active sites.

The reduced C2 catalyst presents higher values of S_{BET} and V_p than C1. These values decrease approximately a 10% during the reaction. The N_2 adsorption–desorption isotherm data indicates that this decrease is due to the reduction of the micro and mesopores. In this case, the coke deposition can be the responsible of the partial blockage of the porous structure. Other authors also proposed that sintering of the Cu and ZnO particles may also lead to

Table 3
Structural parameters of the reduced and used catalysts.

Catalyst	S_{BET} (m^2/g)	V_p (cm^3/g)	r_p [a] (nm)
C1 reduced	14	0.040	5.7
C1 used TOS 217 h	20	0.047	4.7
C1 used TOS 395 h	22	0.064	5.8
C2 reduced	43	0.223	10.4
C2 used TOS 292 h	39	0.198	10.2
C2 used TOS 349 h	37	0.175	9.5
C2 regenerated	43	0.242	11.3

[a] Determined by Wheeler model.

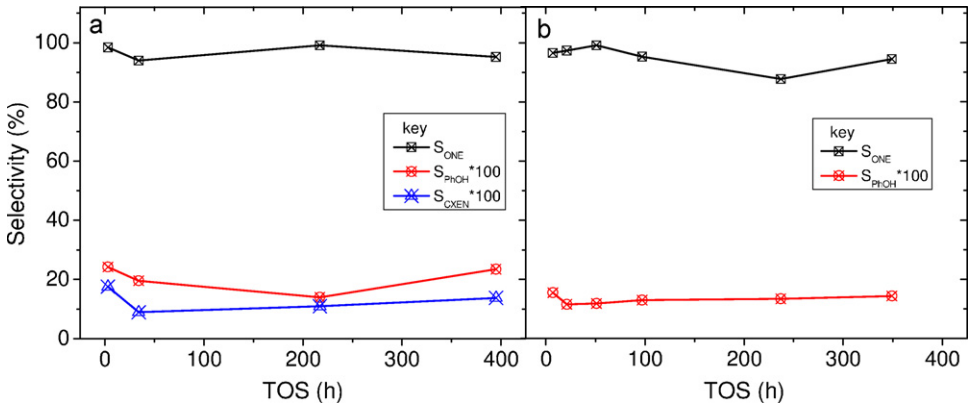

Fig. 6. Yield to cyclohexanone (Y_{ONE}), phenol (Y_{PhOH}) and cyclohexene (Y_{CXEN}), if produced, as a function of TOS for the C1 (a) and C2 (b). T = 250 °C; WHSV = 2.98 h^{-1}.

a decrease in the pore size, and eventually pores close making the active species inaccessible to the reactants [26].

Fig. 5 shows the SEM micrographs of the reduced and used C1 and C2 catalysts, respectively. The morphology of the reduced catalysts is somewhat different from the used catalysts. A non-structured coke seems to be formed on both catalysts after the reaction. The carbonaceous structure deposited on C1 catalyst seems to be heterogeneously deposited, what could slightly increase the porosity of the catalyst. However, in the case of the C2 catalyst, the coke appears more uniformly deposited on the catalysts, decreasing their porosity, in agreement of the N_2 adsorption–desorption data.

3.4. Study of the selectivities

More than 97% of the reacted cyclohexanol produced cyclohexanone. However, other compounds can be obtained by the dehydrogenation and dehydration reaction of cyclohexanol. When cyclohexanone is used as raw material for the production of nylon, these compounds or impurities can strongly affect the fibber properties. Phenol is the most important impurity obtained from the dehydrogenation reaction and it is generated in a slightly major amount by the C2 catalyst. While, cyclohexene is obtained from cyclohexanol dehydration reaction and it can be only observed with the C1 catalyst. The other minority impurities obtained in this reaction for C1 catalyst were water, (directly formed by both dehydration from cyclohexanol to cyclohexene) and a mixture of the isomers 2-cyclohexylidene-cyclohexanone and cyclohexyl-cyclohexanone (from self-condensation of cyclohexanone), and for C2 catalyst was 2-cyclohexen-1-one [14].

These results can be due to the low amount of surface acidic sites on these catalysts, so the dehydration of cyclohexanol is restrained, and the yield of cyclohexanone is high, as can be also deduced by the similarities between cyclohexanol conversion and yield to hydrogen. In this sense, Nagaraja et al. [15] found that the largest amount of chrome in copper chromite catalysts (as this catalyst presents (26%)), can induce dehydrating effects and therefore, it can generate cyclohexene as one of the main impurities.

As aforementioned, these catalysts are very stable under the experimental conditions. In this point, the analysis of the yield with the TOS makes necessary. Fig. 6 reports the yields to cyclohexanone, phenol and cyclohexene (if produced) as a function of TOS for the C1 and C2 catalysts. As can be seen, the yields to the main reaction products remain stable with the TOS, despite the decrease of the activity observed with both catalysts. Even at relatively low activity values, the yield to cyclohexanone is higher than 97%. These results suggest that both the coke deposition and the copper sintering can reduce considerably the cyclohexanol conversion. However, the yield to the desirable product (cyclohexanone) has not been significantly affected by both effects.

3.5. Regeneration

The reactivation of the catalysts was carried out using a regeneration method similar to that described by Marchi et al. [27], when the partial deactivation has been caused by the sintering of the copper, could be carried out by different steps: (i) recovery of the original CuO phase by oxidation of the sintered copper particles, and (ii) regeneration of the Cu^+ phase by reduction with the hydrogen-containing mixture. The treatment in air and hydrogen would therefore redisperse the sintered Cu^+ phase, leading to a recovery of the initial catalytic activity. When the main causes of deactivation are derived from the coke deposition, the regeneration of the catalysts could be performed by the carbon burn-off. As the coke deposition was relatively high in these catalysts, the regeneration by gasification of the carbonaceous deposits was evaluated. However, the gasification of the carbon at high temperatures can produce the copper sintering in these catalysts. Therefore it is advisable to carry out this regeneration at temperatures lower than 350 °C.

In order to determine if the observed deactivation is reversible or irreversible, we tried one regeneration procedure based on the following steps: treatment in air at 300 °C for 8 h, followed by reduction in H_2 (100%) at 300 °C for 8 h. Afterwards, the regenerated catalysts were tested in the gas-phase cyclohexanol dehydrogenation at 250 °C and WHSV = 2.98 h^{-1}.

With this treatment, the carbon content was notably decreased from 7.67 to 0.47% for C1 and from 5.64 to 0.11% for C2, respectively. Therefore, the gasification of the catalysts produced an almost complete removal of the carbonaceous deposits. In this sense, the structural parameters of the regenerated C2 catalysts were analyzed, obtaining the same apparent surface area of the fresh catalyst, what suggests that the initial porosity is totally released. As can be seen in Fig. 2, the XRD profiles of the regenerated catalysts were not noticeable affected by the gasification reaction. However, a 20% increase of the copper crystallite size to 43.5 nm was observed in C1. In the case of C2, the copper crystallite size was not significantly influenced by the regeneration process.

Fig. 7 shows a comparison of the cyclohexanol conversion before and after the regeneration step for C1 (a) and C2 (b) catalysts, at 250 °C and WSHV = 2.98 h^{-1}. The results indicate that the regeneration process was successfully applied and the recovery of the initial cyclohexanol conversions was observed in both catalysts. Nevertheless, a significant decay on the activity was obtained for both catalysts. The cyclohexanol conversion decreases very fast in C1 to finally reach a steady-state conversion value of 30% at TOS higher

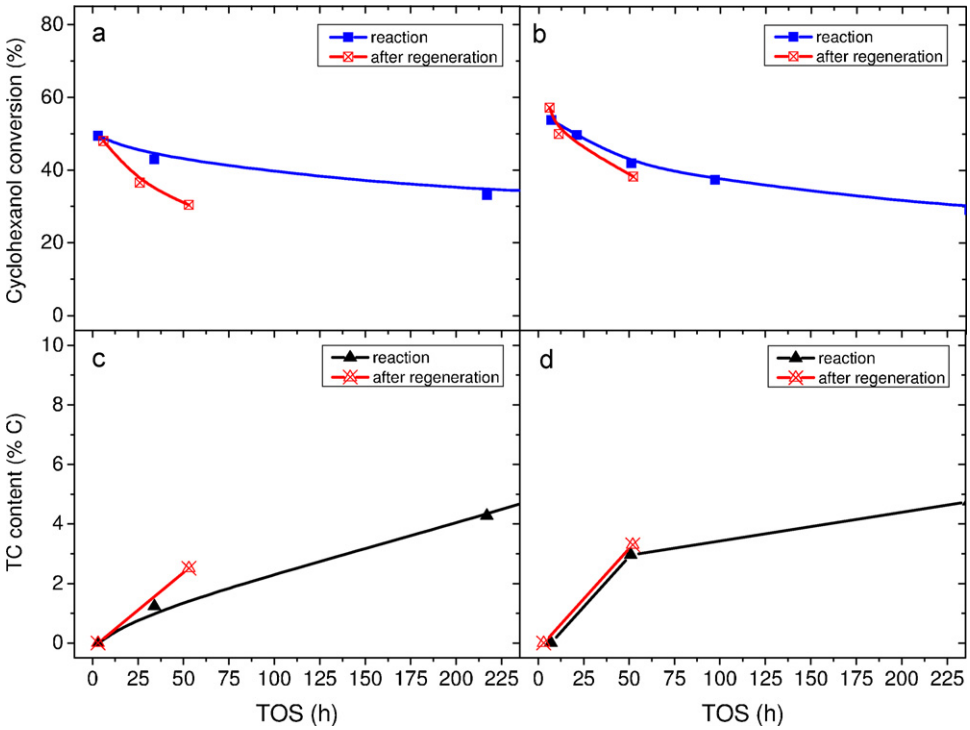

Fig. 7. Evolution of cyclohexanol (X_{OL}) conversion of C1 (a) and C2 (b) and total carbon content of C1 (c) and C2 (d) as a function of TOS, before and after regeneration, at 250 °C and a WHSV = 2.98 h^{-1}.

than 50 h (450 h, if considered the time previous to the regeneration process). This value corresponds to the same one observed previous to the gasification reaction. The decrease on the conversion observed takes place simultaneously to an important increase of the carbon content (to 2.5%). The decay on the activity observed in C2 takes place more slowly, being the cyclohexanol conversions in the range of TOS evaluated similar to the ones obtained before the regeneration process. In this case, the carbon content also increases to 3.3%.

The yield to cyclohexanone for both catalysts remains the same after the regeneration process, indicating that the nature of the active sites is not appreciably modified during the gasification reaction. These results suggest that a regeneration of the catalysts is initially possible due to the removal of the carbonaceous deposits. However, a fast decay on the activity takes place in both catalysts, suggesting that the increase of the copper crystallite size can present some influence on the conversion decrease.

4. Conclusions

Both catalysts tested present high cyclohexanol conversion. A slow deactivation of the catalysts was observed during the reaction, obtaining an activity reduction of the 50% at 400 h. Yield higher than 97% for the cyclohexanol reaction to cyclohexanone was obtained for both catalysts, in all the range of time on stream studied. The main impurities observed were phenol, obtained from the dehydrogenation reaction, and cyclohexene, only observed with the copper chromite catalysts, and derived from the cyclohexanol dehydration. The values of stability and yield for the cyclohexanol dehydrogenation are much higher than others reported in the literature; what could make them very suitable for an industrial application.

The characterization of the catalysts indicated the presence of crystallographic phases of metallic copper, with copper dispersion between 3 and 9%. However, an increase of the crystallite size of metallic copper was observed after the reaction. XRD and SEM analysis evidenced the presence of coke deposited at high time on stream. While, the simultaneous decrease of the relative copper concentration and the increase of the carbon concentration (determined by XPS analysis) suggest that coke deposition takes places preferentially over the copper active sites. Therefore, the main causes of the activity loss observed for these catalysts can be associated to the coke deposition over the copper active sites and the increase of the copper metallic crystallite size. Besides, in the case of the copper zinc oxide catalyst, a slight blockage of the porous structure after the reaction can be observed, probably due to the coke deposition, which can, in addition, diminish the catalyst activity, limiting the accessibility of the reactants to the pores. The regeneration of the catalysts by carbon burn-off removes the carbonaceous deposits. This gasification treatment does not produce any significant modification on the nature of the active sites, because the same yield to cyclohexanone was obtained after this regeneration treatment.

Acknowledgements

The authors acknowledge financial support for this research from the Spanish Ministry of Science and Innovation under projects CTM 2006-00317 and PET 2008-0130. The authors would like to express their gratitude to UBE Corporation Europe S.A. for its support, as well as Süd-Chemie AG for providing the catalyst.

References

[1] H.A. Wittcof, B.G. Reuben, Industrial Organic Chemical, John Wiley & Sons, Inc., 1996, pp. 253–264.
[2] A.H. Cumberley, M.B. Mueller, J. Am. Chem. Soc. 63 (1947) 1535–1536.
[3] Ch. Sivaraj, B. Mahipal Reddy, P.K. Rao, Appl. Catal. 45 (1988) L11–L14.
[4] D.V. Cesar, C.A. Pérez, V.M.M. Salim, M. Schmal, Appl. Catal. A: Gen. 176 (1999) 205–212.
[5] V.Z. Fridman, A.A. Davydov, J. Catal. 195 (2000) 20–30.
[6] V.Z. Fridman, A.A. Davydov, J. Catal. 208 (2002) 497–498.
[7] V.Z. Fridman, A.A. Davydov, K. Titievsky, J. Catal. 222 (2004) 545–557.
[8] M.V. Twigg, Catalyst Handbook, 2nd ed., Wolfe, 1989 (Chapter 6).
[9] C.-Y. Shiau, Y.R. Lee, Appl. Catal. A: Gen. 220 (2001) 173–180.
[10] J.M. Campos-Martin, A. Guerreo-Ruiz, J.L.G. Fierro, J. Catal. 156 (1995) 209–212.

[11] B.J. Liaw, Y.Z. Chen, Appl. Catal. A: Gen. 206 (2001) 245–256.
[12] G. Krishna Reddy, K.S. Rama Rao, P. Kanta Rao, Catal. Lett. 59 (1999) 157–160.
[13] A. Romero, P. Yustos, A. Santos, Ind. Eng. Chem. Res. 42 (2003) 3654–3661.
[14] A. Romero, A. Santos, D. Escrig, E. Simón, Appl. Catal. A: Gen. 392 (2011) 19–27.
[15] B.M. Nagaraja, V. Siva Kumar, V. Shashikala, A.H. Padmasri, S. Sreevardhan Reddy, B. David Raju, K.S. Rama Rao, J. Mol. Catal. A: Chem. 223 (2004) 339–345.
[16] M.V. Twigg, M.S. Spencer, Appl. Catal. A: Gen. 212 (2001) 161–174.
[17] K.V.R. Chary, G.V. Sagar, C.S. Srikanth, V.V. Rao, J. Phys. Chem. B 111 (2007) 543–550.
[18] Z. Wang, J. Xi, W. Wang, G. Lu, J. Mol. Catal. A: Chem. 191 (2003) 123.
[19] A. Fonseca, P. Zeuthen, J.B. Nagy, Fuel 75 (1996) 1363–1376.
[20] R.H. Meinhold, D.M. Bibby, Zeolites 10 (1990) 121–130.
[21] A.R. Pradhan, J.F. Wu, S.J. Jong, T.C. Tsai, S.B. Liu, Appl. Catal. A: Gen. 165 (1997) 489–497.
[22] G. Bai, H. Wang, H. Ning, F. He, G. Chen, React. Kinet. Catal. Lett. 94 (2008) 375–383.
[23] D. Ji, W. Zhe, Z. Wang, G. Wang, Catal. Commun. 8 (2007) 1891–1895.
[24] G. Li, L. Hu, J.M. Hill, Appl. Catal. A: Gen. 301 (2006) 16–24.
[25] J.A. Rodriguez, J.Y. Kim, J.C. Hanson, M. Perez, A.I. Frenkel, Catal. Lett. 85 (2003) 247–254.
[26] H. Wang, L. Chen, G. Bai, D. Luan, Y. Li, X. Yan, Y. Zhang, J. Xing, Catal. Commun. 8 (2007) 145–149.
[27] A.J. Marchi, J.L.G. Fierro, J. Santamaria, A. Monzon, Appl. Catal. A: Gen. 142 (1996) 375–386.